

Computational Design of Multitargeted Ligands to Counter Drug Resistance of *Mycobacterium Tuberculosis*



Varalakshmi Vummidi^{1,*}  and Sekhar Talluri¹ 

¹Department of Biotechnology, GITAM School of Technology, GITAM, Gandhi Nagar, Rushikonda-530045, Visakhapatnam, Andhra Pradesh, India

Abstract:

Background: Tuberculosis (TB) is a significant global health challenge due to drug resistance. Furthermore, tuberculous meningitis (TBM), which affects the central nervous system, has a particularly high mortality rate. TBM drugs have low efficacy because of their low blood-brain barrier (BBB) permeability. Many institutions that treat tuberculosis lack the infrastructure to identify specific drug-resistance mutations. The development of drugs with the capability of treating multiple strains would contribute considerably to the advancement of TB control in countries with limited resources. Therefore, there is an urgent requirement for novel therapeutics that can target native and drug-resistant strains.

Objective: This study aimed to design a novel drug to target native as well as drug-resistant *Mycobacterium tuberculosis* (MTB) strains associated with pulmonary TB and TBM.

Methods: RNA Polymerase beta-subunit (rpoB) was chosen because it is a validated target for MTB. Pharmacophore features, core moiety analysis, and docking scores were used for ligand screening. Deep neural networks (DeepFrag) were used for structural optimization, and binding affinity was evaluated using AutoDock Vina. Custom scoring schemes, STWMM for TB and STWMMM for TBM, met the requirements of high binding affinity for multiple targets, optimal pharmacokinetic profiles, and chemical synthesizability.

Results: M1, M2, and M3 were the molecules with the highest STWMM and STWMMM scores, indicating their potential for TB and TBM therapy. The average binding energy of M1 was -8.83 kcal/mol for native and mutant rpoB. The average binding energy for M2 and M3 was -9.63 and -9.83 kcal/mol, respectively).

Conclusion: In this study, novel ligands for native and drug-resistant TB and TBM therapy were obtained by multi-target drug design. A major challenge for current therapeutic regimens for TB and TBM is the rise of drug-resistant strains of *Mycobacterium tuberculosis* and the necessity of distinguishing them from the native strains. The multitargeted ligands developed in this study have the potential to overcome these limitations.

Keywords: *Mycobacterium tuberculosis*, Tuberculous meningitis, Multitarget drug design, Drug resistance, BBB permeability, Docking, RpoB mutants.

© 2025 The Author(s). Published by Bentham Open.

This is an open access article distributed under the terms of the Creative Commons Attribution 4.0 International Public License (CC-BY 4.0), a copy of which is available at: <https://creativecommons.org/licenses/by/4.0/legalcode>. This license permits unrestricted use, distribution, and reproduction in any medium, provided the original author and source are credited.

*Address correspondence to this author at the Department of Biotechnology, GITAM School of Technology, GITAM, Gandhi Nagar, Rushikonda-530045, Visakhapatnam, Andhra Pradesh, India; E-mail: vummidi@gitam.edu

Cite as: Vummidi V, Talluri S. Computational Design of Multitargeted Ligands to Counter Drug Resistance of *Mycobacterium Tuberculosis*. Open Med Chem J, 2025; 19: e18741045367943. <http://dx.doi.org/10.2174/0118741045367943250203071653>



Received: November 09, 2024

Revised: January 03, 2025

Accepted: January 07, 2025

Published: February 04, 2025



Send Orders for Reprints to reprints@benthamscience.net

1. INTRODUCTION

Tuberculosis (TB) is one of the deadliest infectious diseases, competing with AIDS and malaria [1, 2]. Despite being a preventable and curable illness, tuberculosis remains a primary cause of global mortality and morbidity. In 2022, tuberculosis was the second leading cause of death from a single infectious pathogen, surpassed only by COVID-19. It claimed about twice as many lives as HIV/AIDS, demonstrating its public health impact [3]. RNA polymerase beta-subunit (rpoB) plays a critical role in transcription and is essential for the survival of *Mycobacterium tuberculosis*. Its extremely conserved structure and its role in essential bacterial functions further support the selection of rpoB as an attractive and critical target for therapeutic intervention [4-6]. RpoB is the target of rifampicin, one of the most efficient first-line anti-TB agents. The mutations occurring in this well-characterized gene are by far the most significant cause of rifampicin resistance and are a major barrier to therapy in multidrug-resistant (MDR) and extensively drug-resistant (XDR) cases. The design strategy presented in this work aims to overcome the challenge of drug resistance across a broad spectrum of MTB strains, including those involved in tuberculous meningitis (TBM), by designing inhibitors that bind effectively to native and mutant rpoBs. This multi-target approach has the potential to overcome the limitations of the current TB and TBM therapies.

Tuberculous meningitis (TBM), a severe manifestation that affects the central nervous system, is associated with high rates of morbidity and mortality [7, 8]. It is caused by *Mycobacterium tuberculosis* and can result in a variety of neurological problems if not treated on time [9, 10]. TBM mortality rates can exceed 50%, especially in cases in which the illness is not detected early [11]. This burden worsens in individuals who are co-infected with HIV and have drug-resistant strains of tuberculosis [12, 13]. TBM is a complicated disease that poses a significant challenge to global health. Therefore, improving treatment outcomes requires an understanding of the underlying mechanisms of TBM, particularly those linked to drug resistance [14-16].

Tuberculous meningitis causes clinical problems with a wide range of symptoms, such as fever, headache, altered mental status, and neurological abnormalities [10]. The acid-fast bacilli (AFB) smear test is one example of a traditional diagnostic technique that has low sensitivity, especially in countries with limited resources where it is most frequently used [17, 18]. More sensitive diagnostic methods, such as the GeneXpert MTB/RIF, have been widely adopted. However, availability is still restricted in many high-burden areas, resulting in a large number of untreated or unconfirmed cases [19-21].

The current first-line therapy for tuberculosis, recommended by WHO, includes rifampicin, isoniazid, pyrazinamide, and ethambutol [22]. Although this therapeutic regimen is effective for pulmonary TB, its effectiveness is substantially reduced for MDR-TB [23].

Rifampicin (RMP) is a key component of TB treatment, targeting the RNA polymerase enzyme, specifically the

beta-subunit encoded by the rpoB gene [24, 25]. Concerning patterns in medication resistance to tuberculosis have been reported by recent epidemiological research, especially in rifampicin-resistant strains of the disease that include mutations in the RNA polymerase beta-subunit [26-28]. Comprehending the resistance mechanisms facilitated by these mutations is crucial in order to develop focused therapies that enhance the management of TBM [29].

It has been reported that the most common mutations (65-86%) occur at positions 451 and 456 of rpoB. The emergence of RIF-resistant strains, harboring mutations, such as S456L, H451D, H451P, H451Y, and D441V within the RNA polymerase beta-subunit, poses a significant obstacle to effective TB treatment [30-32]. The effectiveness of the drug is decreased by these mutations because they alter the RIF binding site on RNA polymerase. Treatment becomes even more challenging due to *M. tuberculosis's* tendency to develop fitness-compensatory mutations [33]. By enabling the resistant strains to survive and replicate even in the absence of the medication, these changes can lessen the fitness costs associated with drug resistance, extending the duration of resistant bacterial populations in the host and the community [34, 35]. Developing innovative therapies against tuberculosis (TB) by targeting the RNA polymerase beta-subunit is a potential path, particularly when considering drug-resistant strains [36, 37].

RpoB mutations are present in 96.1% of RIF-resistant MTB strains globally [38-40]. Most of the drug resistance strains have mutations in the Rifampicin Resistance Determining Region (RRDR), which is found close to the active site amino acid residues 432-458 (amino acids 507-533 according to *E.coli* numbering) of RNA polymerase beta-subunit. These mutations are also found in TBM, which affects the efficacy of treatment methods [41, 42]. A study in India found the presence of drug-resistant mutations in TBM patients, highlighting the challenge of managing drug-resistant TBM [43]. A study in South Africa revealed a high frequency of multi-drug-resistant (MDR) TB strains in TB cases, with rpoB mutations at positions 451 and 456 playing a key role [44].

Resistance mutations are not only confined to rpoB but also include changes in other genes, such as katG and inhA, which are implicated in isoniazid activation and function [45-48]. The prevalence of resistant mutants differs by geographic region and population [49, 50]. Isoniazid activation requires the katG gene, which encodes catalase-peroxidase. Mutations in katG can cause isoniazid resistance. According to reports, katG mutations are common in multidrug-resistant (MDR) TB strains and occur in a large proportion of TB patients [51]. Approximately 30% of MDR-TB cases have katG mutations, which complicate treatment regimens. Mutations in inhA lead to isoniazid resistance and are present in around 15-20% of resistant TB strains.

Besides rpoB, katG, and inhA, mutations in genes like embB and pncA have been related to resistance to ethambutol and pyrazinamide, respectively [52-54]. Although

less common, these mutations add to the overall complexity of TB treatment.

Drugs, such as bedaquiline, pretomanid, linezolid, and moxifloxacin, which are novel drugs with different targets, have been shown to be more effective than the current first-line therapeutic regimen for MDR-TB [55]. However, since drug resistance may develop for these novel drugs also, the usage of the new drugs is only recommended for cases where resistance to the first-line therapeutic regimen is confirmed [56]. Identification of drug resistance based on lack of response may lead to undesirable irreversible consequences in some cases, and many institutions that are responsible for the treatment of TB do not have the facilities to determine the drug resistance profile. The goal of this work is to design multitargeted drugs that are effective against native rpoB as well as the common mutants that confer drug resistance to *Mycobacterium tuberculosis* so that they can be prescribed as a replacement for rifampicin without knowledge of the state of drug resistance.

The *Mycobacterium tuberculosis* (MTB) rpoB mutants (S456L, H451D, H451P, H451Y, and D441V) were chosen for this study based on their reported role in mediating drug resistance. Numerous reports have linked these changes to resistance to rifampicin, one of the major antibiotics used in combating tuberculosis (TB). Although these changes are frequently seen in pulmonary tuberculosis (TB), there is growing evidence that drug-resistant strains are also associated with tuberculous meningitis (TBM) [11, 57, 58].

Research indicates that TBM cases reflect the same drug-resistance mechanisms as pulmonary tuberculosis, with rpoB gene mutations being a major factor in reducing the efficacy of conventional therapies [59, 60]. This is a serious problem for the management of TBM since drug resistance can seriously impair the effectiveness of current treatment methods [61]. It is important to address these rpoB mutations in order to develop novel therapeutic approaches, particularly for drug-resistant cases of TBM when traditional therapies may not be effective.

In this study, *in silico* approaches were utilized to design novel therapeutic agents to target rpoB and its mutants. Deep neural networks, molecular docking, and advanced scoring schemes were used to design, screen, and rank potential drug candidates based on their predicted binding affinity and efficacy against TB and TBM. The objective of this study was to design multitargeted ligands for effective treatment of drug-susceptible and drug-resistant *M. tuberculosis* strains to improve the treatment outcomes for patients with pulmonary TB as well as TBM.

2. METHODOLOGY

2.1. Target Preparation

Although seventy-one structures of rpoB of *Mycobacterium tuberculosis* are available in the RCSB PDB, these experimentally obtained structures are either of low resolution that is not adequate for accurate computational docking studies or structural information regarding some fragments is missing. Therefore, the structure of the native

molecular target, rpoB, was obtained from the AlphaFold server known for its high-accuracy predictions of protein structures from amino acid sequences [62]. This structure was used as the reference for our docking studies. For the drug-resistant mutants of rpoB, including S456L, H451D, H451P, H451Y, and D441V, the mutant models were generated using the Robetta server [63], which is capable of generating 3D protein structures with high accuracy. AutoDock Tools (ADT), an extensively used and validated software package for preparing docking simulations, was utilized to process the receptor structures, which involved the removal of water molecules, the addition of polar hydrogens, and the selection of rotatable bonds. All side chains in the receptor structure were defined as non-rotatable.

2.2. Ligand Preparation

2.2.1. Initial Screening

A set of 2041 natural product molecules (sourced from www.selleckchem.com) were screened for binding affinity against the rpoB S456L mutant protein using AutoDock4 [64]. For each molecule, AutoDockTools were used to prepare it as a 3D structure with the required atom types, charge assignments, and hydrogen addition. Then, all these prepared ligands were subjected to docking using AutoDock 4. Each ligand was docked into the active sites of mutant rpoB protein, and the docking pose binding energy for each ligand was recorded.

2.2.2. Identification of Binding Site Pockets

AutoDock Tools were used to define the binding site pockets of rpoB S456L. The grid box was centered over a predicted site of activity on the rpoB S456L mutant, which was identified in earlier studies on the native RNA polymerase beta subunit. The grid was selected to be large enough to include the main catalytic site but also the secondary binding pockets. A 0.375 Å spacing in the grid was selected, meeting demands for precision with computational efficiency. This box served as the docking area for the virtual screening, ensuring that only relevant conformations of the ligands were considered for further analysis.

2.2.3. Screening Process

Each of the 2041 natural product molecules was subjected to virtual screening within the defined site pockets. The Lamarckian genetic algorithm was applied for the docking simulations. This algorithm explores ligand conformations within the binding site, optimizing the ligand's orientation and conformation to find the lowest-energy binding mode. Each molecule was docked multiple times to ensure the consistency of results. After docking, ligands were ranked based on their binding energy and their interactions with key residues in the pocket. The top-scoring molecules were selected for further analysis.

Following screening, the core moiety structures of the top-docked molecules were analyzed by using Avogadro [65], a molecular editing and visualization software. It was used to examine the three-dimensional structures, analyze molecular interactions, and identify key functional groups that could influence binding affinity and pharmacokinetic

properties. This structural analysis led to the design of 32 novel molecules. The ADME (Absorption, Distribution, Metabolism, and Excretion) properties of these molecules were assessed by using SWISS-ADME [66]. The BBB permeability of the molecules was assessed using the PKCSM (<https://biosig.lab.uq.edu.au/pkcsm/>) [67] tool to determine their ability to cross the blood-brain barrier, which is crucial for potential central nervous system (CNS) therapeutics.

2.2.4. Advanced Docking

From the initial screening, 32 molecules were chosen based on their binding energies and interactions with the *rpoB* S456L mutant. These molecules were docked into the active site of the *rpoB* S456L mutant protein using AutoDock Vina [68], which was employed for precise binding energy calculations. A grid box for docking was prepared with the active site at the center, with dimensions of 66 x 74 x 72 Å and grid spacing of 0.375 Å by using AutoDock Tools. The docking output, consisting of 10 conformers and their affinity scores, was visualized by using Pymol. These 10 molecules were further docked with *rpoB* and the following drug-resistant mutants of *rpoB*: D441V, H451D, H451P, and H451Y.

2.2.5. Optimization with DeepFrag

To further enhance the binding affinity of the identified molecules, the top 10 molecules were subjected to optimization using DeepFrag (<https://durrantlab.pitt.edu/deepfrag/>) [69], a deep learning-based fragment optimization tool. This optimization process involved generating and evaluating novel molecular fragments to improve binding scores and refine interactions with the target proteins. This integrated approach facilitated the design and optimization of 100 novel molecules, combining computational screening, detailed docking with binding energy calculations, and advanced fragment optimization to identify and refine potential therapeutics for targeting *rpoB* mutants. From the 100 molecules designed and optimized through this integrated approach, the top 10 molecules were selected based on their superior binding affinity, chemical synthesizability, favorable ADME properties, and effective BBB permeability.

2.3. Scoring Scheme

The AutoDock Vina scoring function was employed to evaluate the binding affinity of each ligand. Vina's scoring function estimates the free energy of binding based on ligand-receptor interactions, including van der Waals forces, electrostatic interactions, hydrogen bonding, and torsional flexibility. In addition to binding affinity, the pharmacokinetic attributes and chemical synthesizability were included in the scoring function. Lipinski, Ghose, Veber, Egan, and Muegge are logical values that are non-zero for drug-like compounds and were estimated by using the SWISS-ADME server. Lead-likeness is a logical value and is non-zero for lead like ligands estimated by using the SWISS-ADME server. Synthetic accessibility scores (SA) [70] can be calculated from fragment contributions and complexity analysis. In this study, they were obtained using the SWISS-ADME server. SA values range from 1 for easily

synthesizable ligands to 10 for ligands that are very difficult to synthesize. \log_{BB_pkCSM} is a quantitative estimate of BBB permeability obtained by using the pkCSM server. $BBB_{permeability_F}$ is a logical value that is non-zero for ligands predicted to be BBB permeable using the SWISS-ADME server.

2.3.1. STWMM Score

A weighted score, STW score, was calculated to include terms for pharmacokinetics and chemical synthesizability in addition to the AutoDock Vina score. It was calculated using the following formula:

$$STWscore = -0.5 * Vina\ Score + 1.0 * Lipinski_F + 0.125 * Ghose_F + 0.125 * Veber_F + 0.125 * Egan_F + 0.125 * Muegge_F + 1.0 * Bioavailability + 0.5 * Lead-likeness_F + 2.0 * (10 - SA) / 9$$

The last term of the STWscore was designed to have a maximum value of 2.0 for SA=1 and a minimum value of 0 for SA=10. The weights for the STWscore were selected to balance the requirements of affinity (pharmacodynamics), pharmacokinetics, and synthetic accessibility. STWscore is not a normalized score, and there is no maximum or minimum. For an excellent ligand with an AutoDock Vina score of -10.0 kcal/mol, bioavailability of 1.0, and synthetic accessibility of 1, which satisfies all the rules for drug-like molecules, the STWscore will be 10.0, with a 50% score due to binding affinity, 20% from synthetic accessibility, and 30% from other pharmacokinetic properties. Higher scores are possible for molecules with higher affinity.

The STWscore was calculated for each ligand of interest for the native form of the target as well as for each of the mutants. Furthermore, the STWMM score for the ligand was calculated as the *minimum* of the STWscores for the native and mutants that were under consideration, as follows:

$$STWMM\ Score = \text{MIN} \{ \text{Native_STWscore}, \text{S456L_STWscore}, \text{H451D_STWscore}, \text{H451P_STWscore}, \text{H451Y_STWscore}, \text{D441V_STWscore} \}$$

2.3.2. STWNMM Score

A weighted score, STWNscore, was calculated to include terms for BBB permeability, pharmacokinetics, and chemical synthesizability, in addition to the AutoDock Vina score [71].

$$STWNscore = -0.5 * Vina\ Score + \log_{BB_pkCSM} + 0.25 * BBB_{permeability_F} + 1.0 * Lipinski_F + 0.125 * Ghose_F + 0.125 * Muegge_F + 0.5 * Lead-likeness_F + 2.0 * (10 - SA) / 9$$

The last term of STWN score was designed to have a maximum value of 2.0 for SA=1 and a minimum value of 0 for SA=10. The weights for the STWNscore were selected to balance the requirements of affinity (pharmacodynamics), permeability through the BBB, pharmacokinetics, and synthetic accessibility. STWNscore is not a normalized score, and there is no maximum or minimum. For an excellent ligand with an AutoDock Vina score of -10.0 kcal/mol, a \log_{BB} of 1.0, and synthetic accessibility of 1, which is predicted to be BBB permeable and satisfies all the rules for drug-like molecules, the STWNscore will be 10.0,

with 50% of score due to binding affinity, 20% from synthetic accessibility, 12.5% contribution from BBB permeability, and 17.5% from other pharmacokinetic properties. Higher scores are possible for molecules with higher affinity or higher logBB values.

The STWNScore was calculated for each ligand of interest for the native form of the target as well as for each of the mutants. The STWMMM score for the ligand was then calculated as the *minimum* of the STWNScores for the native and mutants that were under consideration, as follows:

$$\text{STWMMM score} = \text{MIN} \{ \text{Native_STWNScore}, \text{S456L_STWNScore}, \text{H451D_STWNScore}, \text{H451P_STWNScore}, \text{H451Y_STWNScore}, \text{D441V_STWNScore} \}$$

2.4. Visualization and Plotting

ChemDraw was used to create 2D representations of the designed ligands [72], PyMOL was used for visualization and plotting of the ligand-target interactions [73], and the PLIP server was used for analysis and visualization of molecular interactions [74].

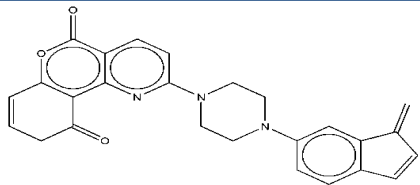
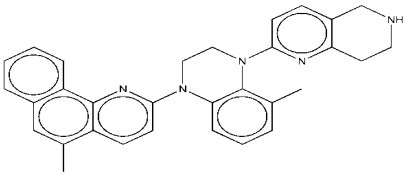
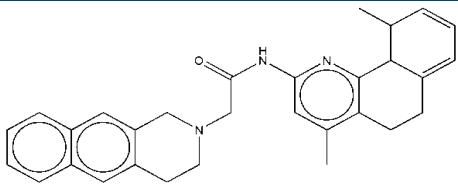
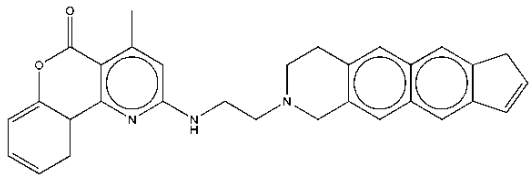
3. RESULTS

AutoDock Vina is a widely used open-source software for molecular docking, developed to predict the binding mode and affinity of small molecules to their target pro-

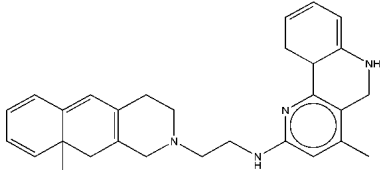
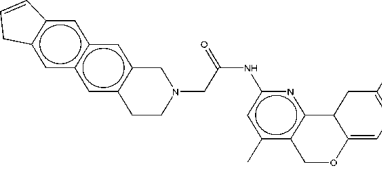
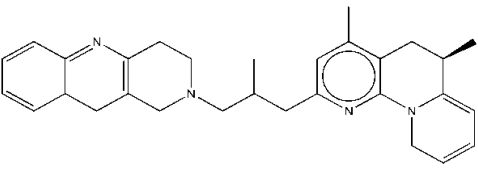
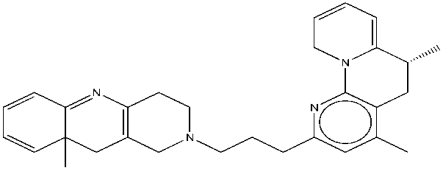
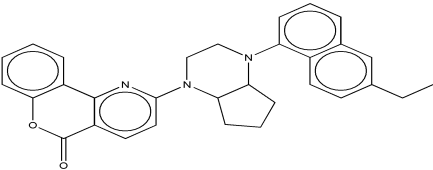
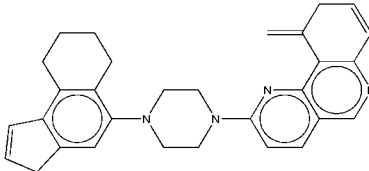
teins. AutoDock Vina uses a scoring function, which, in turn, depends on various parameters like van der Waals interactions, electrostatic interactions, hydrogen bonding, desolvation effects, *etc.*, to estimate the free energy of binding, *i.e.*, docking energy, which is a crucial parameter in evaluating the potential of a molecule as a drug candidate. This energy is expressed in kilocalories per mole (kcal/mol). A more negative value indicates a stronger and more favorable interaction between the ligand and the target. Free energy of binding of -8.5 kcal or better (more negative) indicates a high affinity of the ligand for the protein [75-77].

The blood-brain barrier (BBB) is a selective, semi-permeable barrier that separates the circulating blood from the brain's extracellular fluid in the central nervous system (CNS). It serves as a critical checkpoint, protecting the brain from potentially harmful substances while allowing essential nutrients to pass through it [78]. For drugs intended to treat neurological conditions, the ability to cross the BBB is a vital consideration in drug design. LogBB is the log of the ratio of the concentration of the ligand in the brain to its concentration in the blood. Ligands with logBB > 0.3 are generally able to cross the blood-brain barrier, while molecules with logBB < -1 have poor access to the brain [67]. All the designed ligands, reported in Table 1, have a logBB value greater than 0.3.

Table 1. STWMM and STWMMM scores and synthetic accessibility of the designed ligands.

S.No.	Molecule Name	Structure	STWMM Score	STWMMM Score	Swiss-ADME Synthetic Accessibility
1	M1		7.51	7.37	4.04
2	M2		7.48	7.56	3.8
3	M3		7.45	7.38	4.82
4	M4		7.30	7.15	4.89

(Table 1) contd....

S.No.	Molecule Name	Structure	STWMM Score	STWMMM Score	Swiss-ADME Synthetic Accessibility
5	M5		7.24	7	5.25
6	M6		7.21	7.01	4.89
7	M7		7.15	7.02	5.89
8	M8		6.91	6.75	5.7
9	M9		6.84	6.78	4.47
10	M10		6.69	6.5	4.2

The evaluation of novel therapeutic molecules targeting RNA polymerase mutants was conducted using two distinct scoring schemes: the STWMMM score, which focuses on drug-resistant mutations (DRMs) relevant to tuberculous meningitis, and the STWMM score, which encompasses DRMs in *Mycobacterium tuberculosis* (general). The top ten molecules based on their STWMM score are presented in Table 1. The AutoDock Vina scores of designed ligands for the native and rpoB mutant targets are presented in Table 2.

The binding energies reflect the interactions between the ligands and the target proteins, which are crucial for evaluating the therapeutic potential of these compounds against native and drug-resistant *Mycobacterium tuberculosis*. The data reported in Table 2 show that the designed molecules, M1-M7, have a binding energy of -8.5 kcal/mol or better for native as well as for all the mutants of rpoB that were included in this study. M8 has a binding energy of -8.5 kcal/mol or better for native and for all the mutants that were included in this study, except against the mutant target

H451Y (-8.05 kcal/mol). M9 and M10 have a binding energy of -8.5 kcal/mol or better for native and for all the mutants that were included in this study, except against the mutant targets H451Y and H451P.

Table 1 presents the STWMM scores, STWMMM scores, and synthetic accessibility for the top ten designed ligands targeting the native RNA polymerase beta subunit and mutants observed in drug-resistant strains of *Mycobacterium tuberculosis*. As mentioned in Table 1, the top three molecules are M1, M2, and M3 based on their STWMM scores.

Molecule M1, with the highest STWMM score of 7.51, shows an average AutoDock Vina score of -8.83 kcal/mol. This suggests a favorable binding affinity across different mutants, indicating its potential as a strong candidate for further development. Specifically, its binding energies range from -8.52 kcal/mol to -9.51 kcal/mol, demonstrating consistency in binding across the S456L, H451D, H451P,

Table 2. Binding energies of designed ligands for native and mutant rpoB proteins.

S.No.	Molecule Name	AutoDock Vina Score (kcal/mol)						Average AutoDock Vina Score (kcal/mol)
		Rpob2	S456L	H451D	H451P	H451Y	D441V	
1	M1	-8.84	-9.51	-8.63	-8.87	-8.59	-8.52	-8.83
2	M2	-9.87	-10.92	-9.02	-9.14	-8.6	-10.24	-9.63
3	M3	-10.4	-10.44	-10.31	-9.33	-9.0	-9.49	-9.83
4	M4	-10.37	-10.67	-10.05	-9.52	-8.73	-9.02	-9.73
5	M5	-9.75	-10.59	-9.95	-9.82	-8.52	-8.93	-9.59
6	M6	-9.81	-11.25	-9.19	-8.55	-8.94	-8.93	-9.45
7	M7	-10.18	-10.05	-9.55	-9.29	-8.63	-9.44	-9.52
8	M8	-9.15	-10.1	-10.02	-9.65	-8.05	-9.98	-9.49
9	M9	-9.59	-9.25	-8.68	-7.62	-8.47	-8.77	-8.73
10	M10	-9.17	-9.95	-8.86	-7.21	-8.12	-8.86	-8.70

H451Y, and D441V mutants. The high STWMM score, high STWMMM score, and the high binding affinity of M1 position it as a lead compound in the pursuit of new therapeutics for pulmonary tuberculosis as well as for tuberculous meningitis.

The interactions of molecule M1 with the active site of rpoB are illustrated in Fig. (1). M1 forms a hydrogen bond with Q614, and this interaction is critical for stabilizing the ligand within the binding pocket. Thus, this bond makes a significant contribution to the binding affinity of this ligand. There are two additional hydrogen bonds in this complex. One involves R613, which forms a medium-strength hydrogen bond, and another involves R454, which forms a weaker

hydrogen bond. In addition to the formation of the hydrogen bond, R613 also forms a salt bridge to a carboxylate group in the ligand. In addition to these interactions, R613 stabilizes this complex through π -cation interactions. Hydrophobic interactions with V176, Q435, L436, L458, P489, and Q614 further stabilize the overall ligand-receptor complex, especially within the hydrophobic pocket of rpoB. These interactions firmly anchor the M1 molecule within the active site. The combination of hydrogen bonding, electrostatic, and hydrophobic interactions indicates that there is a strong possibility that M1 may retain tight binding against a variety of mutations, which is a prime concern in dealing with drug-resistant variants.

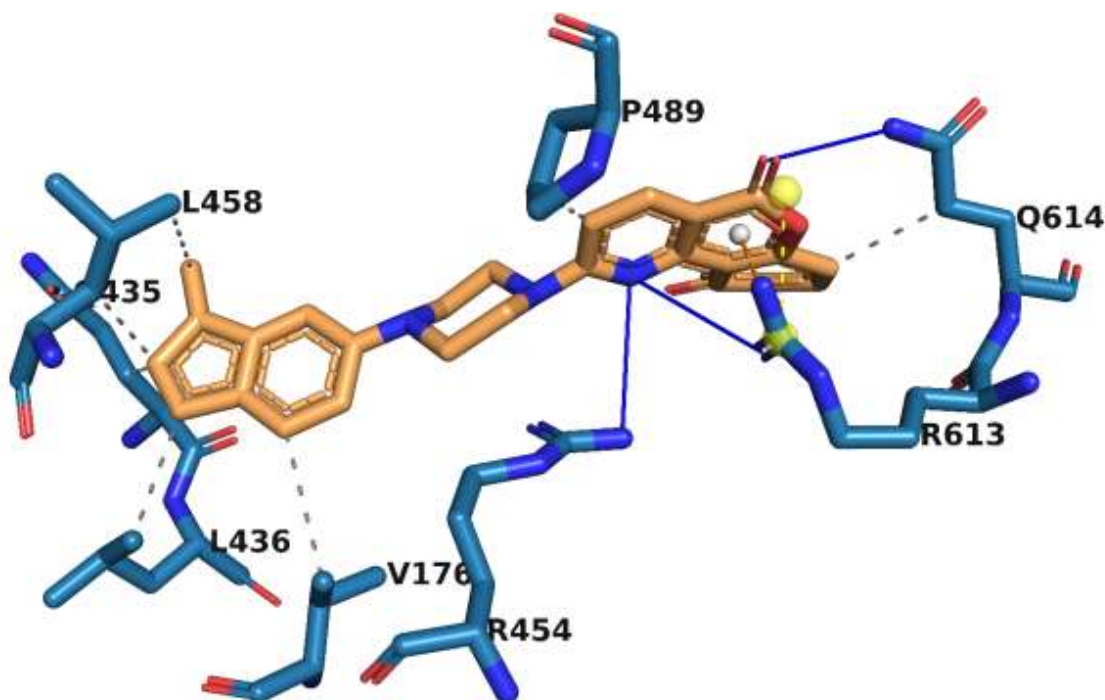


Fig. (1). Interaction of molecule M1 with the active site residues of rpoB protein. The blue lines represent hydrogen bonds, the yellow dashed lines represent salt bridges, the orange dashed lines represent π -cation interactions, and the grey dashed lines represent hydrophobic interactions.

Molecule M2 exhibits an average binding energy of -9.63 kcal/mol, indicating it has one of the highest affinity among the designed compounds. Its individual binding scores, ranging from -8.60 kcal/mol to -10.92 kcal/mol, indicate that M2 has a high binding affinity for native rpoB as well as for all the mutants that were included in this study. The exceptional binding affinity of M2 indicates its potential as a therapeutic agent for TB and TBM. The slightly lower STWMM score of M2, compared to M1, indicates that M1 has better pharmacokinetic properties. However, the STWMMM score of M2 is higher than that of M1, indicating that it has better BBB permeability than M1, and hence, it may be more effective for TBM therapy compared to M1. It can be concluded that M2 will be effective for both TB and TBM.

The interactions of molecule M2 within the rpoB active site are shown in Fig. (2). Q435 forms two strong hydrogen bonds with M2. These interactions play a significant role in the stabilization of the rpoB-M2 complex. π -cation interactions of the ligand with R454 further stabilize this complex. The ligand is anchored in the hydrophobic segment of the active site through its hydrophobic interactions with V176 and D441. In addition, weak van der Waal's interactions with numerous residues in the active site stabilize this complex. The stabilization of this complex by numerous interactions indicates that the binding of M2 would be robust with respect to minor changes caused by point mutations in the target.

Molecule M3 has the best average AutoDock Vina score of -9.83 kcal/mol. The binding energies of M3, ranging from -9 kcal/mol to -10.4 kcal/mol, predict that it has a high binding affinity for native rpoB as well as for all the mutants

that were included in this study, indicating that it is a potential candidate for drug development. Its consistent performance across the mutants reinforces its potential role in addressing resistance in combating drug-resistant *Mycobacterium tuberculosis*. Molecule M3 is ranked third for TB and second for TBM. The STWMM and STWMMM scores for M3 are lower than those for M1 and M2 because they have higher synthetic accessibility scores.

The binding interactions of molecule M3 to the active site of rpoB are illustrated in Fig. (3). M3 forms two strong hydrogen bonds with the backbone of F439, which is important because the backbone interactions are less prone to disruption from point mutations than interactions involving side chains. Binding of this nature by the backbone enables multitargeting, and it indicates the possibility that M3 could be active against a large number of rpoB mutants, including the most common resistance-associated mutations. M3 forms another strong hydrogen bond with R454. A salt bridge between D441 and a tertiary amine group in the ligand further stabilizes this complex. A strong hydrophobic interaction with F439 and additional hydrophobic interactions with Q438 and N679 firmly anchor M3 within the active site. The backbone hydrogen bond with F439 is a particularly strategic interaction for drug design, as it is less prone to alteration by mutations, which are a frequent cause of drug resistance. The diversity of non-covalent interactions, including van der Waals forces from multiple residues, increases binding affinity and makes this ligand resilient to structural variations induced by point mutation. Hence, M3 is a promising candidate for the treatment of drug-resistant strains of *M. tuberculosis*.

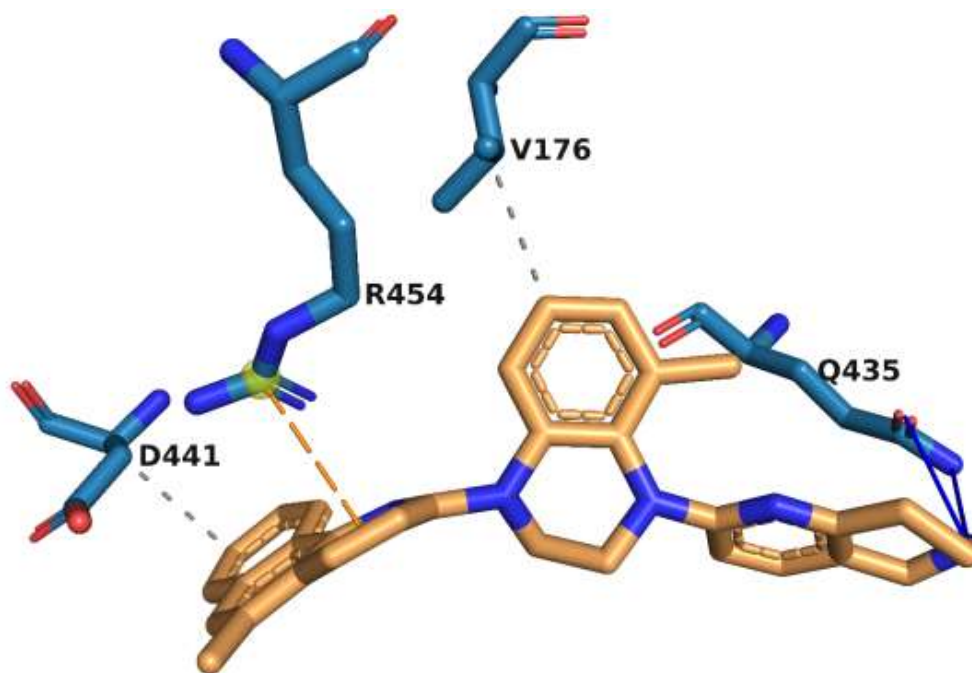


Fig. (2). Interaction of molecule M2 with the active site residues of rpoB protein. The blue lines represent hydrogen bonds, the orange dashed lines represent π -cation interactions, and the grey dashed lines represent hydrophobic interactions.

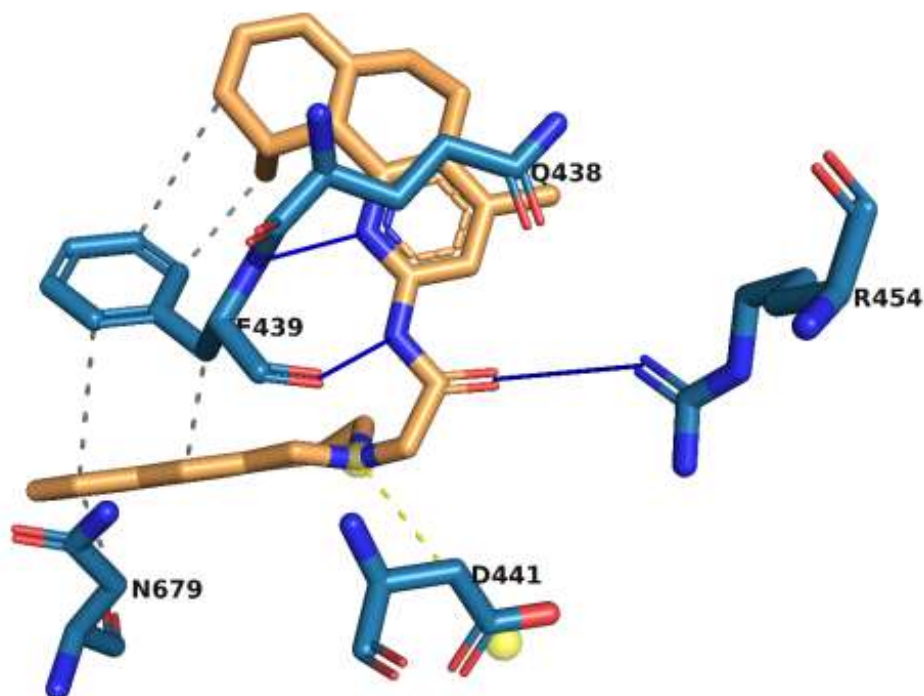


Fig. (3). Interaction of molecule M3 with the active site residues of rpoB protein. The blue lines represent hydrogen bonds, the yellow dashed lines represent salt bridges, and the grey dashed lines represent hydrophobic interactions.

4. DISCUSSION

The first line of therapy, consisting of rifampicin, isoniazid, pyrazinamide, and ethambutol, recommended by WHO, is effective for the treatment of pulmonary tuberculosis [79]. However, this therapeutic protocol has a much lower efficacy for tuberculous meningitis because all components of this selected set have a low permeability through the blood-brain-barrier. Rifampicin has a pkCSM-logBB value of -2.1. The corresponding logBB values for isoniazid, pyrazinamide, and ethambutol are 0.00, -0.01, and -0.21, respectively, indicating that they are also expected to have low permeability through the BBB. Similarly, the new drugs developed for the treatment of pulmonary TB also have very low values of logBB . For example, bedaquiline, delamanid, and pretomanid have pkCSM-logBB values of 0.03, -2.1, and -1.7, respectively, indicating poor BBB permeability. All the designed ligands reported in Table 1 of this work have pkCSM-logBB values higher than 0.3, indicating adequate permeability through the BBB and the potential for higher efficacy of treatment for TBM. Customized drug delivery agents, such as nanoparticles, are being investigated to improve the permeability of rifampicin and isoniazid to improve the outcomes for tuberculous meningitis [80]. Drug resistance mutations have also decreased the efficacy of the first line of therapy. The BV-BRC database [81] includes descriptions of 25054 MTB strains resistant to rifampicin, 22022 MTB strains resistant to isoniazid, 2363 MTB strains resistant to pyrazinamide, and 9283 MTB strains resistant to ethambutol. Several novel drugs have been developed to overcome the drug resistance problem. However, these drugs are also susceptible to development of drug resis-

tance. For example, 25 MTB strains resistant to bedaquiline and 571 MTB strains resistant to delamanid have been documented in the BV-BRC database. Although multiple-medication therapy, consisting of a combination of drugs, can be utilized, it can lead to undesirable adverse effects. The optimization of dosage and duration of each component is more complicated for drug combinations than for single drugs. The design of a single drug that has a high affinity for multiple targets provides an alternative solution that is potentially more efficient [82]. Multitargeted agents have been developed for the treatment of infectious diseases, such as malaria and Chagas disease [83, 84]. Designing poly-functional drugs is difficult using conventional methods. However, several computational strategies for the design of poly-functional drugs have been proposed, such as fragment-based design [85]. Our approach for multitargeted drug design is also fragment-based, but the utilization of Deep Neural Networks has resulted in a substantial increase in the efficiency of the design process [69].

Rifampicin is one of the most effective therapeutics for pulmonary TB. However, the emergence of mutations in its target, the RNA polymerase beta subunit (rpoB), has greatly reduced its effectiveness. These mutations cause major changes to the rifampicin-binding site, lowering the drug's ability to suppress RNA synthesis, which is necessary for bacterial replication [86-88]. This study's major goal is to provide an effective therapeutic option for both pulmonary TB and tuberculous meningitis (TBM) by designing novel multitargeted ligands whose effectiveness would not be reduced by such mutations. In this study, we

conducted an *in silico* design of novel ligands targeting RNA polymerase and its mutants.

TBM is a particularly severe form of tuberculosis involving infection of the central nervous system. TBM therapy requires the design of drugs that penetrate the blood-brain barrier (BBB), which is a very challenging problem [89, 90]. Current TB drugs, which have been developed primarily for pulmonary tuberculosis, frequently fail to permeate the BBB in sufficient concentrations to effectively combat TBM [91, 92]. This limitation emphasizes the importance of developing drugs that are not only effective against drug-resistant strains of *M. tuberculosis* but are also capable of crossing the BBB to treat central nervous system infections. This work is intended to generate such ligands by targeting rpoB and its mutations, with the goal of reducing the high mortality rate due to TBM.

RpoB was selected as the molecular target due to its involvement in bacterial transcription and because it has been validated as a target of Rifampicin, which is one of the most effective drugs against TB. Mutations in the Rifampicin Resistance-Determining Region (RRDR), including S456L, H451D, H451P, H451Y, and D441V, were chosen due to their high frequency in clinical isolates and their effect on rifampicin efficacy [93-95]. These mutations alter the rifampicin binding pocket of rpoB, lowering rifampicin binding affinity and, in many cases, resulting in a high level of drug resistance. The core moiety analysis, performed with Avogadro, was very important in refining the ligands' structural components. By identifying the most significant molecular fragments responsible for high-affinity binding, we were able to concentrate on ligands capable of overcoming the steric and electronic alterations caused by rpoB mutations. This level of structural insight is crucial. After preliminary screening, we used DeepFrag to design novel ligands. DeepFrag uses machine learning techniques to recommend changes to small compounds that improve their binding properties while preserving or improving their pharmacokinetic properties. This enabled a more in-depth exploration of the chemical structures, resulting in the discovery of molecules with increased binding potential for rpoB and its mutants.

Balancing the activity of the designed ligands, against the multiple targets of interest is critical to ensure that a high dose would not be required to ensure efficacy against all targets of interest [96]. The STWMM and STWMMM scoring schemes were developed to assess the ligands' potential efficacy against pulmonary tuberculosis and TBM, respectively. These scoring schemes include the most important criteria for effective drugs, integrating binding affinity, mutational resistance, pharmacokinetics, and chemical synthetic accessibility to provide a complete framework for evaluating the therapeutic potential of designed molecules. These scoring schemes were designed to address the problem that arises when the dominant variant of the pathogen is eliminated by the utilization of an antibiotic and the niche initially occupied by the drug-susceptible strain is rapidly occupied by a mutant that is initially present at low frequency in the initial population. The multi-targeted ligands selected by the STWMM and

STWMMM scoring schemes ensure that the ligands with high STWMM and STWMMM scores have high efficacy against the native as well as against all the drug-resistant strains. In addition, since the designed multi-targeted ligands are effective against both the native and mutant strains, the importance of obtaining genotyping information, or for other tests of drug resistance, is less than that for conventional drugs.

This study goes beyond the computational aspects of drug design to highlight the broader consequences of targeting rpoB mutations. The prevalence of these mutations in clinical isolates of drug-resistant *M. tuberculosis* emphasizes the relevance of focusing on these targets in future treatment approaches. The S456L mutation, for example, has been shown to confer high-level resistance across a variety of geographic regions, making it an important target for therapeutic development. Similarly, changes like H451D and D441V complicate the treatment landscape since they not only provide resistance but also modify bacterial fitness, potentially allowing resistant strains to survive and spread.

Moreover, the challenges posed by TBM add an additional layer of complexity to TB treatment. TBM is associated with high mortality, particularly in regions with limited access to diagnostic tools and effective treatments. The ability of the designed ligands to cross the BBB and maintain efficacy in the central nervous system is a critical advancement. The study's dual focus on both pulmonary TB and TBM reflects the real-world need for therapeutics that can address the diverse clinical manifestations of tuberculosis. Future experimental validation of these designed ligands is critical for ensuring their efficacy and safety. Expanding this approach to include other mutations and targets of other drugs could further enhance our ability to combat drug-resistant *Mycobacterium tuberculosis*.

CONCLUSION

In this study, we successfully designed novel multi-targeted ligands as potential drugs for pulmonary TB and TBM. The designed ligands have a high affinity for both native as well as for mutant rpoB of *Mycobacterium tuberculosis*. Our approach involved molecular docking-based screening and ranking and deep neural network (DeepFrag) based optimization. We also examined how well these molecules might pass through the blood-brain barrier by calculating pkCSM BBB values, which is particularly important for the treatment of TBM, which affects the central nervous system. In addition, we assessed synthetic accessibility by using Swiss-ADME to ensure that these molecules could be produced efficiently. AutoDock Vina was employed to evaluate binding affinity for the native and mutant forms of rpoB (S456L, H451D, H451P, H451Y, and D441V), which are involved in resistance to current treatments for TB. Moreover, the designed molecules were assessed using novel scoring schemes, STWMM and STWMMM, that were designed for integrated assessment of the essential features desired in drugs, such as binding affinity, mutational resistance, pharmacokinetics, and synthesizability.

After a thorough analysis, three promising candidates,

M1, M2, and M3, were identified. Each of these designed molecules was predicted to possess favorable pharmacokinetics, chemical synthesizability, and a high binding affinity towards native rpoB, as well as against all mutant variants that were included in this study. Based on these promising results, we conclude that the designed multitargeted molecules, M1, M2, and M3, offer a new treatment option for TB and TBM, especially in cases where drug resistance is a concern. Further *in vitro* and *in vivo* studies are warranted to confirm their effectiveness and potential for clinical use.

In conclusion, this study represents a significant step forward in addressing the urgent need for developing novel therapeutic approaches for TB and TBM by designing ligands with the capability to target both native and mutant strains of *Mycobacterium tuberculosis*.

AUTHORS' CONTRIBUTION

V.V. and S.T.: Provided the conception and design of the study; V.V.: Collected the data, analyzed the data, and wrote the manuscript; S.T.: Assisted in target preparation, manuscript editing, and revision.

LIST OF ABBREVIATIONS

TB	= Tuberculosis
TBM	= Tuberculous Meningitis
CNS	= Central Nervous System
HIV	= Human Immunodeficiency Virus
rpoB	= RNA Polymerase beta-subunit
RMP	= Rifampicin
AFB	= Acid-Fast Bacilli
RRDR	= Rifampicin Resistance Determining Region
ADME	= Absorption, Distribution, Metabolism, and Excretion
BBB	= Blood-Brain Barrier
MTB	= <i>Mycobacterium tuberculosis</i>
MDR	= Multidrug-Resistant

ETHICS APPROVAL AND CONSENT TO PARTICIPATE

Not applicable.

HUMAN AND ANIMAL RIGHTS

Not applicable.

CONSENT FOR PUBLICATION

Not applicable.

AVAILABILITY OF DATA AND MATERIALS

All data generated or analysed during this study are included in this article.

FUNDING

None.

CONFLICT OF INTEREST

The authors declare no conflict of interest, financial or otherwise.

ACKNOWLEDGEMENTS

Declared none.

REFERENCES

- [1] Orgeur, M.; Sous, C.; Madacki, J.; Brosch, R. Evolution and emergence of *Mycobacterium tuberculosis*. *FEMS Microbiol. Rev.*, **2024**, *48*(2), fuae006. <http://dx.doi.org/10.1093/femsre/fuae006> PMID: 38365982
- [2] Silke, F.; Earl, L.; Hsu, J.; Janko, M.M.; Joffe, J.; Memetova, A.; Michael, D.; Zheng, P.; Aravkin, A.; Murray, C.J.L.; Weaver, M.R. Cost-effectiveness of interventions for HIV/AIDS, malaria, syphilis, and tuberculosis in 128 countries: A meta-regression analysis. *Lancet Glob. Health*, **2024**, *12*(7), e1159-e1173. [http://dx.doi.org/10.1016/S2214-109X\(24\)00181-5](http://dx.doi.org/10.1016/S2214-109X(24)00181-5) PMID: 38876762
- [3] *Global tuberculosis report*; World Health Organization: Geneva, **2023**, pp. 1-6.
- [4] Dookie, N.; Rambaran, S.; Padayatchi, N.; Mahomed, S.; Naidoo, K. Evolution of drug resistance in *Mycobacterium tuberculosis*: A review on the molecular determinants of resistance and implications for personalized care. *J. Antimicrob. Chemother.*, **2018**, *73*(5), 1138-1151. <http://dx.doi.org/10.1093/jac/dkx506> PMID: 29360989
- [5] Lange, C.; Abubakar, I.; Alffenaar, J.W.C.; Bothamley, G.; Caminero, J.A.; Carvalho, A.C.C.; Chang, K.C.; Codecasa, L.; Correia, A.; Crudu, V.; Davies, P.; Dedicoat, M.; Drobniewski, F.; Duarte, R.; Ehlers, C.; Erkens, C.; Goletti, D.; Günther, G.; Ibraim, E.; Kampmann, B.; Kuku, L.; de Lange, W.; van Leth, F.; van Lunzen, J.; Matteelli, A.; Menzies, D.; Monedero, I.; Richter, E.; Rüsck-Gerdes, S.; Sandgren, A.; Scardigli, A.; Skrahina, A.; Tortoli, E.; Volchenkov, G.; Wagner, D.; van der Werf, M.J.; Williams, B.; Yew, W.W.; Zellweger, J.P.; Cirillo, D.M. Management of patients with multidrug-resistant/extensively drug-resistant tuberculosis in Europe: A TBNET consensus statement. *Eur. Respir. J.*, **2014**, *44*(1), 23-63. <http://dx.doi.org/10.1183/09031936.00188313> PMID: 24659544
- [6] Seung, K.J.; Keshavjee, S.; Rich, M.L. Multidrug-resistant tuberculosis and extensively drug-resistant tuberculosis. *Cold Spring Harb. Perspect. Med.*, **2015**, *5*(9), a017863. <http://dx.doi.org/10.1101/cshperspect.a017863> PMID: 25918181
- [7] Török, M.E. Tuberculous meningitis: Advances in diagnosis and treatment. *Br. Med. Bull.*, **2015**, *113*(1), 117-131. <http://dx.doi.org/10.1093/bmb/ldv003> PMID: 25693576
- [8] Heemskerk, A.D.; Nguyen, M.T.H.; Dang, H.T.M.; Vinh Nguyen, C.V.; Nguyen, L.H.; Do, T.D.A.; Nguyen, T.T.T.; Wolbers, M.; Day, J.; Le, T.T.P.; Nguyen, B.D.; Caws, M.; Thwaites, G.E. Clinical outcomes of patients with drug-resistant tuberculous meningitis treated with an intensified antituberculosis regimen. *Clin. Infect. Dis.*, **2017**, *65*(1), 20-28. <http://dx.doi.org/10.1093/cid/cix230> PMID: 28472255
- [9] Arshad, A.; Dayal, S.; Gadhe, R.; Mawley, A.; Shin, K.; Tellez, D.; Phan, P.; Venketaraman, V. Analysis of tuberculosis meningitis pathogenesis, diagnosis, and treatment. *J. Clin. Med.*, **2020**, *9*(9), 2962. <http://dx.doi.org/10.3390/jcm9092962> PMID: 32937808
- [10] Marx, G.E.; Chan, E.D. Tuberculous meningitis: Diagnosis and treatment overview. *Tuberc. Res. Treat.*, **2011**, *2011*, 1-9. <http://dx.doi.org/10.1155/2011/798764> PMID: 22567269
- [11] Evans, E.E.; Avaliani, T.; Gujabidze, M.; Bakuradze, T.; Kipiani, M.; Sabanadze, S. Long term outcomes of patients with tuberculous meningitis: The impact of drug resistance. *PLoS One*, **2022**, *17*(6), e0270201. <http://dx.doi.org/10.1371/journal.pone.0270201> PMID: 35749509

- [12] Boyles, T.; Locatelli, I.; Senn, N.; Ebell, M. Determining clinical decision thresholds for HIV-positive patients suspected of having tuberculosis. *Evid. Based Med.*, **2017**, 22(4), 132-138. <http://dx.doi.org/10.1136/ebmed-2017-110718> PMID: 28716809
- [13] Koole, O.; Thai, S.; Khun, K.E.; Pe, R.; Van Griensven, J.; Apers, L. Evaluation of the 2007 WHO guideline to improve the diagnosis of tuberculosis in ambulatory HIV-positive adults. *PLoS One*, **2011**, 6(4), e18502. <http://dx.doi.org/10.1371/journal.pone.0018502> PMID: 21494694
- [14] Imran, D.; Hill, P.C.; McKnight, J.; van Crevel, R. Establishing the cascade of care for patients with tuberculous meningitis. *Wellcome Open Res.*, **2019**, 4, 177. <http://dx.doi.org/10.12688/wellcomeopenres.15515.1> PMID: 32118119
- [15] Wilkinson, R.J.; Rohlwink, U.; Misra, U.K.; van Crevel, R.; Mai, N.T.H.; Dooley, K.E.; Caws, M.; Figaji, A.; Savic, R.; Solomons, R.; Thwaites, G.E. Tuberculous meningitis. *Nat. Rev. Neurol.*, **2017**, 13(10), 581-598. <http://dx.doi.org/10.1038/nrneuro.2017.120> PMID: 28884751
- [16] Purohit, M.R.; Purohit, R.; Mustafa, T. Patient Health Seeking and Diagnostic Delay in Extrapulmonary Tuberculosis: A Hospital Based Study from Central India. *Tuberc. Res. Treat.*, **2019**, 2019, 1-8. <http://dx.doi.org/10.1155/2019/4840561> PMID: 30854235
- [17] Bahr, N.C.; Meintjes, G.; Boulware, D.R. Inadequate diagnostics: The case to move beyond the bacilli for detection of meningitis due to *Mycobacterium tuberculosis*. *J. Med. Microbiol.*, **2019**, 68(5), 755-760. <http://dx.doi.org/10.1099/jmm.0.000975> PMID: 30994435
- [18] Bahr, N.C.; Tugume, L.; Rajasingham, R.; Kiggundu, R.; Williams, D.A.; Morawski, B.; Alland, D.; Meya, D.B.; Rhein, J.; Boulware, D.R. Improved diagnostic sensitivity for tuberculous meningitis with Xpert® MTB/RIF of centrifuged CSF. *Int. J. Tuberc. Lung Dis.*, **2015**, 19(10), 1209-1215. <http://dx.doi.org/10.5588/ijtld.15.0253> PMID: 26459535
- [19] Seddon, J.A.; Tugume, L.; Solomons, R.; Prasad, K.; Bahr, N.C. The current global situation for tuberculous meningitis: Epidemiology, diagnostics, treatment and outcomes. *Wellcome Open Res.*, **2019**, 4, 167. <http://dx.doi.org/10.12688/wellcomeopenres.15535.1> PMID: 32118118
- [20] Nhu, N.T.Q.; Heemskerk, D.; Thu, D.D.A.; Chau, T.T.H.; Mai, N.T.H.; Nghia, H.D.T.; Loc, P.P.; Ha, D.T.M.; Merson, L.; Thinh, T.T.V.; Day, J.; Chau, N.V.; Wolbers, M.; Farrar, J.; Caws, M. Evaluation of GeneXpert MTB/RIF for diagnosis of tuberculous meningitis. *J. Clin. Microbiol.*, **2014**, 52(1), 226-233. <http://dx.doi.org/10.1128/JCM.01834-13> PMID: 24197880
- [21] Denkinger, C.M.; Schumacher, S.G.; Boehme, C.C.; Dendukuri, N.; Pai, M.; Steingart, K.R. Xpert MTB/RIF assay for the diagnosis of extrapulmonary tuberculosis: A systematic review and meta-analysis. *Eur. Respir. J.*, **2014**, 44(2), 435-446. <http://dx.doi.org/10.1183/09031936.00007814> PMID: 24696113
- [22] Hall, R.G., II; Leff, R.D.; Gumbo, T. Treatment of active pulmonary tuberculosis in adults: Current standards and recent advances. *Pharmacotherapy*, **2009**, 29(12), 1468-1481. <http://dx.doi.org/10.1592/phco.29.12.1468> PMID: 19947806
- [23] Prasad, R.; Gupta, N.; Banka, A. Multidrug-resistant tuberculosis/rifampicin-resistant tuberculosis: Principles of management. *Lung India*, **2018**, 35(1), 78-81. http://dx.doi.org/10.4103/lungindia.lungindia_98_17 PMID: 29319042
- [24] Sheng, J.; Li, J.; Sheng, G.; Yu, H.; Huang, H.; Cao, H.; Lu, Y.; Deng, X. Characterization of *rpoB* mutations associated with rifampin resistance in *Mycobacterium tuberculosis* from eastern China. *J. Appl. Microbiol.*, **2008**, 105(3), 904-911. <http://dx.doi.org/10.1111/j.1365-2672.2008.03815.x> PMID: 18422555
- [25] Goldstein, B.P. Resistance to rifampicin: A review. *J. Antibiot. (Tokyo)*, **2014**, 67(9), 625-630. <http://dx.doi.org/10.1038/ja.2014.107> PMID: 25118103
- [26] Theron, G.; Zijenah, L.; Chanda, D.; Clowes, P.; Rachow, A.; Lesosky, M.; Bara, W.; Mungofa, S.; Pai, M.; Hoelscher, M.; Dowdy, D.; Pym, A.; Mwaba, P.; Mason, P.; Peter, J.; Dheda, K. Feasibility, accuracy, and clinical effect of point-of-care Xpert MTB/RIF testing for tuberculosis in primary-care settings in Africa: A multicentre, randomised, controlled trial. *Lancet*, **2014**, 383(9915), 424-435. [http://dx.doi.org/10.1016/S0140-6736\(13\)62073-5](http://dx.doi.org/10.1016/S0140-6736(13)62073-5) PMID: 24176144
- [27] Kumar, S.; Jena, L. Understanding rifampicin resistance in tuberculosis through a computational approach. *Genomics Inform.*, **2014**, 12(4), 276-282. <http://dx.doi.org/10.5808/GI.2014.12.4.276> PMID: 25705170
- [28] Mani, C.; Selvakumar, N.; Narayanan, S.; Narayanan, P.R. Mutations in the *rpoB* gene of multidrug-resistant *Mycobacterium tuberculosis* clinical isolates from India. *J. Clin. Microbiol.*, **2001**, 39(8), 2987-2990. <http://dx.doi.org/10.1128/JCM.39.8.2987-2990.2001> PMID: 11474030
- [29] Singh, A.; Grover, S.; Sinha, S.; Das, M.; Somvanshi, P.; Grover, A. Mechanistic principles behind molecular mechanism of rifampicin resistance in mutant rna polymerase beta subunit of *Mycobacterium tuberculosis*. *J. Cell. Biochem.*, **2017**, 118(12), 4594-4606. <http://dx.doi.org/10.1002/jcb.26124> PMID: 28485504
- [30] Zaw, M.T.; Emran, N.A.; Lin, Z. Mutations inside rifampicin-resistance determining region of *rpoB* gene associated with rifampicin-resistance in *Mycobacterium tuberculosis*. *J. Infect. Publ. Heal.*, **2018**, 11(5), 605-610. <http://dx.doi.org/10.1016/j.jiph.2018.04.005> PMID: 29706316
- [31] Unissa, A.N.; Hassan, S.; Kumari, V.I.; Revathy, R.; Hanna, L.E. Insights into RpoB clinical mutants in mediating rifampicin resistance in *Mycobacterium tuberculosis*. *J. Mol. Graph. Model.*, **2016**, 67, 20-32. <http://dx.doi.org/10.1016/j.jmglm.2016.04.005> PMID: 27155814
- [32] Rukasha, I.; Said, H.M.; Omar, S.V.; Koornhof, H.; Dreyer, A.W.; Musekiwa, A.; Moultrie, H.; Hoosen, A.A.; Kaplan, G.; Fallows, D.; Ismail, N. Correlation of *rpoB* mutations with minimal inhibitory concentration of rifampin and rifabutin in *Mycobacterium tuberculosis* in an HIV/AIDS endemic setting, South Africa. *Front. Microbiol.*, **2016**, 7, 1947. <http://dx.doi.org/10.3389/fmicb.2016.01947> PMID: 27994580
- [33] Mariam, D.H.; Mengistu, Y.; Hoffner, S.E.; Andersson, D.I. Effect of *rpoB* mutations conferring rifampin resistance on fitness of *Mycobacterium tuberculosis*. *Antimicrob. Agents Chemother.*, **2004**, 48(4), 1289-1294. <http://dx.doi.org/10.1128/AAC.48.4.1289-1294.2004> PMID: 15047531
- [34] Hughes, D.; Brandis, G. Rifampicin resistance: Fitness costs and the significance of compensatory evolution. *Antibiotics (Basel)*, **2013**, 2(2), 206-216. <http://dx.doi.org/10.3390/antibiotics2020206> PMID: 27029299
- [35] Ruslami, R.; Ganiem, A.R.; Aarnoutse, R.E.; van Crevel, R. Rifampicin and moxifloxacin for tuberculous meningitis - Authors' reply. *Lancet Infect. Dis.*, **2013**, 13(7), 570. [http://dx.doi.org/10.1016/S1473-3099\(13\)70156-7](http://dx.doi.org/10.1016/S1473-3099(13)70156-7) PMID: 23809224
- [36] Koch, A.; Mizrahi, V.; Warner, D.F. The impact of drug resistance on *Mycobacterium tuberculosis* physiology: What can we learn from rifampicin? *Emerg. Microbes Infect.*, **2014**, 3(1), 1-11. <http://dx.doi.org/10.1038/emi.2014.17> PMID: 26038512
- [37] Campbell, E.A.; Korzheva, N.; Mustae, A.; Murakami, K.; Nair, S.; Goldfarb, A.; Darst, S.A. Structural mechanism for rifampicin inhibition of bacterial rna polymerase. *Cell*, **2001**, 104(6), 901-912. [http://dx.doi.org/10.1016/S0092-8674\(01\)00286-0](http://dx.doi.org/10.1016/S0092-8674(01)00286-0) PMID: 11290327
- [38] Mboowa, G.; Namaganda, C.; Ssengooba, W. Rifampicin

- resistance mutations in the 81 bp RRDR of rpoB gene in *Mycobacterium tuberculosis* clinical isolates using Xpert®MTB/RIF in Kampala, Uganda: A retrospective study. *BMC Infect. Dis.*, **2014**, *14*(1), 481.
<http://dx.doi.org/10.1186/1471-2334-14-481> PMID: 25190040
- [39] Ramaswamy, S.; Musser, J.M. Molecular genetic basis of antimicrobial agent resistance in *Mycobacterium tuberculosis*: 1998 update. *Tuber Lung Dis.*, **1998**, *79*(1), 3-29.
<http://dx.doi.org/10.1054/tuld.1998.0002> PMID: 10645439
- [40] Singh, P.; Jamal, S.; Ahmed, F.; Saqib, N.; Mehra, S.; Ali, W.; Roy, D.; Ehtesham, N.Z.; Hasnain, S.E. Computational modeling and bioinformatic analyses of functional mutations in drug target genes in *Mycobacterium tuberculosis*. *Comput. Struct. Biotechnol. J.*, **2021**, *19*, 2423-2446.
<http://dx.doi.org/10.1016/j.csbj.2021.04.034> PMID: 34025934
- [41] Yam, W.C.; Tam, C.M.; Leung, C.C.; Tong, H.L.; Chan, K.H.; Leung, E.T.Y.; Wong, K.C.; Yew, W.W.; Seto, W.H.; Yuen, K.Y.; Ho, P.L. Direct detection of rifampin-resistant *Mycobacterium tuberculosis* in respiratory specimens by PCR-DNA sequencing. *J. Clin. Microbiol.*, **2004**, *42*(10), 4438-4443.
<http://dx.doi.org/10.1128/JCM.42.10.4438-4443.2004> PMID: 15472290
- [42] Sinha, P.; Srivastava, G.N.; Tripathi, R.; Mishra, M.N.; Anupurba, S. Detection of mutations in the rpoB gene of rifampicin-resistant *Mycobacterium tuberculosis* strains inhibiting wild type probe hybridization in the MTBDR plus assay by DNA sequencing directly from clinical specimens. *BMC Microbiol.*, **2020**, *20*(1), 284.
<http://dx.doi.org/10.1186/s12866-020-01967-5> PMID: 32938393
- [43] Krishnakumariam, K.; Ellappan, K.; Muthuraj, M.; Tamilarasu, K.; Kumar, S.V.; Joseph, N.M. Molecular diagnosis, genetic diversity and drug sensitivity patterns of *Mycobacterium tuberculosis* strains isolated from tuberculous meningitis patients at a tertiary care hospital in South India. *PLoS One*, **2020**, *15*(10), e0240257.
<http://dx.doi.org/10.1371/journal.pone.0240257> PMID: 33017455
- [44] Dookie, N.; Sturm, A.W.; Moodley, P. Mechanisms of first-line antimicrobial resistance in multi-drug and extensively drug resistant strains of *Mycobacterium tuberculosis* in KwaZulu-Natal, South Africa. *BMC Infect. Dis.*, **2016**, *16*(1), 609.
<http://dx.doi.org/10.1186/s12879-016-1906-3> PMID: 27784282
- [45] Moaddab, S.R.; Farajnia, S.; Kardan, D.; Zamanlou, S.; Alikhani, M.Y. Isoniazid MIC and KatG gene mutations among *Mycobacterium tuberculosis* isolates in Northwest of Iran. *Iran J. Basic Med. Sci.*, **2011**, *14*(6), 540-545.
PMID: 23493326
- [46] Vilch e, C.; Jacobs, W.R., Jr Resistance to isoniazid and ethionamide in *Mycobacterium tuberculosis*: Genes, mutations, and causalities. *Microbiol. Spectr.*, **2014**, *2*(4), MGM2-0014-2013.
<http://dx.doi.org/10.1128/microbiolspec.MGM2-0014-2013> PMID: 26104204
- [47] Reta, M.A.; Maningi, N.E.; Fourie, P.B. Patterns and profiles of drug resistance-conferring mutations in *Mycobacterium tuberculosis* genotypes isolated from tuberculosis-suspected attendees of spiritual holy water sites in Northwest Ethiopia. *Front. Publ. Heal.*, **2024**, *12*, 1356826.
<http://dx.doi.org/10.3389/fpubh.2024.1356826> PMID: 38566794
- [48] Isakova, J.; Sovkhozova, N.; Vinnikov, D.; Goncharova, Z.; Talabekova, E.; Aldasheva, N.; Aldashev, A. Mutations of rpoB, katG, inhA and ahp genes in rifampicin and isoniazid-resistant *Mycobacterium tuberculosis* in Kyrgyz Republic. *BMC Microbiol.*, **2018**, *18*(1), 22.
<http://dx.doi.org/10.1186/s12866-018-1168-x> PMID: 29566660
- [49] Jiao, W.W.; Mokrousov, I.; Sun, G.Z.; Li, M.; Liu, J.W.; Narvsakaya, O. Molecular characteristics of rifampin and isoniazid resistant *Mycobacterium tuberculosis* strains from Beijing, China. *Chin. Med. J. (Engl)*, **2007**, *120*(9), 814-819.
PMID: 17531124
- [50] Rosales-Klinton, S.; Jureen, P.; Zalutskaya, A.; Skrahina, A.; Xu, B.; Hu, Y.; Pineda-Garcia, L.; Merza, M.A.; Muntean, I.; Bwanga, F.; Jobola, M.; Hoffner, S.E. Drug resistance-related mutations in multidrug-resistant *Mycobacterium tuberculosis* isolates from diverse geographical regions. *Int. J. Mycobacteriol.*, **2012**, *1*(3), 124-130.
<http://dx.doi.org/10.1016/j.ijmyco.2012.08.001> PMID: 26787207
- [51] Somoskovi, A.; Parsons, L.M.; Salfinger, M. The molecular basis of resistance to isoniazid, rifampin, and pyrazinamide in *Mycobacterium tuberculosis*. *Respir. Res.*, **2001**, *2*(3), 164-168.
<http://dx.doi.org/10.1186/rr54> PMID: 11686881
- [52] Bakhtiyariniya, P.; Khosravi, A.D.; Hashemzadeh, M.; Savari, M. Identification of mutations in rpoB, pncA, embB, and ubiA genes among drug-resistant *Mycobacterium tuberculosis* clinical isolates from Iran. *Acta Microbiol. Immunol. Hung.*, **2022**. Advance online publication
<http://dx.doi.org/10.1556/030.2022.01730> PMID: 35452411
- [53] Lety, M.A.; Nair, S.; Berche, P.; Escuyer, V. A single point mutation in the embB gene is responsible for resistance to ethambutol in *Mycobacterium smegmatis*. *Antimicrob. Agents Chemother.*, **1997**, *41*(12), 2629-2633.
<http://dx.doi.org/10.1128/AAC.41.12.2629> PMID: 9420031
- [54] Ando, H.; Kondo, Y.; Suetake, T.; Toyota, E.; Kato, S.; Mori, T.; Kirikae, T. Identification of katG mutations associated with high-level isoniazid resistance in *Mycobacterium tuberculosis*. *Antimicrob. Agents Chemother.*, **2010**, *54*(5), 1793-1799.
<http://dx.doi.org/10.1128/AAC.01691-09> PMID: 20211896
- [55] Oelofse, S.; Esmail, A.; Diacon, A.H.; Conradie, F.; Olayanju, O.; Ngubane, N.; Howell, P.; Everitt, D.; Crook, A.M.; Mendel, C.M.; Wills, G.H.; Oluhosi, M.; del Parigi, A.; Sun, E.; Calatroni, A.; Spigelman, M.; Dheda, K. Pretomanid with bedaquiline and linezolid for drug-resistant TB: A comparison of prospective cohorts. *Int. J. Tuberc. Lung Dis.*, **2021**, *25*(6), 453-460.
<http://dx.doi.org/10.5588/ijtld.21.0035> PMID: 34049607
- [56] Black, T.A.; Buchwald, U.K. The pipeline of new molecules and regimens against drug-resistant tuberculosis. *J. Clin. Tuberc. Other Mycobact. Dis.*, **2021**, *25*, 100285.
<http://dx.doi.org/10.1016/j.jctube.2021.100285> PMID: 34816020
- [57] Wang, T.; Feng, G.D.; Pang, Y.; Liu, J.Y.; Zhou, Y.; Yang, Y.N.; Dai, W.; Zhang, L.; Li, Q.; Gao, Y.; Chen, P.; Zhan, L.P.; Marais, B.J.; Zhao, Y.L.; Zhao, G. High rate of drug resistance among tuberculous meningitis cases in Shaanxi province, China. *Sci. Rep.*, **2016**, *6*(1), 25251.
<http://dx.doi.org/10.1038/srep25251> PMID: 27143630
- [58] Caws, M.; Thwaites, G.E.; Duy, P.M.; Tho, D.Q.; Lan, N.T.; Hoa, D.V.; Chau, T.T.; Huyen, M.N.; Anh, P.T.; Chau, N.V.; Chinh, T.N.; Stepniewska, K.; Farrar, J. Molecular analysis of *Mycobacterium tuberculosis* causing multidrug-resistant tuberculosis meningitis. *Int. J. Tuberc. Lung Dis.*, **2007**, *11*(2), 202-208.
PMID: 17263292
- [59] Duo, L.; Ying, B.; Song, X.; Lu, X.; Ye, Y.; Fan, H.; Xin, J.; Wang, L. Molecular profile of drug resistance in tuberculous meningitis from southwest china. *Clin. Infect. Dis.*, **2011**, *53*(11), 1067-1073.
<http://dx.doi.org/10.1093/cid/cir663> PMID: 22021920
- [60] Gupta, R.; Thakur, R.; Kushwaha, S.; Jalan, N.; Rawat, P.; Gupta, P.; Aggarwal, A.; Gupta, M.; Manchanda, V. Isoniazid and rifampicin heteroresistant *Mycobacterium tuberculosis* isolated from tuberculous meningitis patients in India. *Indian J. Tuberc.*, **2018**, *65*(1), 52-56.
<http://dx.doi.org/10.1016/j.ijtb.2017.08.005> PMID: 29332649
- [61] Garg, R.K.; Jain, A.; Malhotra, H.S.; Agrawal, A.; Garg, R. Drug-resistant tuberculous meningitis. *Expert Rev. Anti Infect. Ther.*, **2013**, *11*(6), 605-621.
<http://dx.doi.org/10.1586/eri.13.39> PMID: 23750732
- [62] Jumper, J.; Evans, R.; Pritzel, A.; Green, T.; Figurnov, M.; Ronneberger, O.; Tunyasuvunakool, K.; Bates, R.;  idek, A.; Potapenko, A.; Bridgland, A.; Meyer, C.; Kohl, S.A.A.; Ballard, A.J.; Cowie, A.; Romera-Paredes, B.; Nikolov, S.; Jain, R.; Adler, J.; Back, T.; Petersen, S.; Reiman, D.; Clancy, E.; Zielinski, M.; Steinegger, M.; Pacholska, M.; Berghammer, T.; Bodenstern, S.;

- Silver, D.; Vinyals, O.; Senior, A.W.; Kavukcuoglu, K.; Kohli, P.; Hassabis, D. Highly accurate protein structure prediction with AlphaFold. *Nature*, **2021**, 596(7873), 583-589.
<http://dx.doi.org/10.1038/s41586-021-03819-2> PMID: 34265844
- [63] Kim, D.E.; Chivian, D.; Baker, D. Protein structure prediction and analysis using the Robetta server. *Nucl. Acids. Res.*, **2004**, 32, W526-W531.
<http://dx.doi.org/10.1093/nar/gkh468> PMID: 15215442
- [64] Morris, G.M.; Huey, R.; Lindstrom, W.; Sanner, M.F.; Belew, R.K.; Goodsell, D.S.; Olson, A.J. AutoDock4 and AutoDockTools4: Automated docking with selective receptor flexibility. *J. Comput. Chem.*, **2009**, 30(16), 2785-2791.
<http://dx.doi.org/10.1002/jcc.21256> PMID: 19399780
- [65] Hanwell, M.D.; Curtis, D.E.; Lonie, D.C.; Vandermeersch, T.; Zurek, E.; Hutchison, G.R. Avogadro: An advanced semantic chemical editor, visualization, and analysis platform. *J. Cheminform.*, **2012**, 4(1), 17.
<http://dx.doi.org/10.1186/1758-2946-4-17> PMID: 22889332
- [66] Daina, A.; Michielin, O.; Zoete, V. SwissADME: A free web tool to evaluate pharmacokinetics, drug-likeness and medicinal chemistry friendliness of small molecules. *Sci. Rep.*, **2017**, 7(1), 42717.
<http://dx.doi.org/10.1038/srep42717> PMID: 28256516
- [67] Pires, D.E.V.; Blundell, T.L.; Ascher, D.B. pkCSM: Predicting small-molecule pharmacokinetic and toxicity properties using graph-based signatures. *J. Med. Chem.*, **2015**, 58(9), 4066-4072.
<http://dx.doi.org/10.1021/acs.jmedchem.5b00104> PMID: 25860834
- [68] Trott, O.; Olson, A.J. AutoDock Vina: Improving the speed and accuracy of docking with a new scoring function, efficient optimization, and multithreading. *J. Comput. Chem.*, **2010**, 31(2), 455-461.
<http://dx.doi.org/10.1002/jcc.21334> PMID: 19499576
- [69] Green, H.; Koes, D.R.; Durrant, J.D. DeepFrag: A deep convolutional neural network for fragment-based lead optimization. *Chem. Sci. (Camb.)*, **2021**, 12(23), 8036-8047.
<http://dx.doi.org/10.1039/D1SC00163A> PMID: 34194693
- [70] Ertl, P.; Schuffenhauer, A. Estimation of synthetic accessibility score of drug-like molecules based on molecular complexity and fragment contributions. *J. Cheminform.*, **2009**, 1(1), 8.
<http://dx.doi.org/10.1186/1758-2946-1-8> PMID: 20298526
- [71] Vummidi, V.; Talluri, S. Design of RNA polymerase inhibitors as therapeutics for tuberculous meningitis. *Infect. Disord. Drug Targ.*, **2024**, 25(3), e18715265341228.
<http://dx.doi.org/10.2174/0118715265341228240827062721>
- [72] Mendelsohn, L.D. ChemDraw 8 sions. *J. Chem. Inf. Comput. Sci.*, **2004**, 44(6), 2225-2226.
<http://dx.doi.org/10.1021/ci401023t>
- [73] Schrödinger, LLC. The PyMOL molecular graphics system, version 1.8. *Amer. J. Infect. Dis. Microbiol.*, **2015**, 4(3), 61-71.
<http://dx.doi.org/10.12691/ajidm-4-3-3>
- [74] Adasme, M.F.; Linnemann, K.L.; Bolz, S.N.; Kaiser, F.; Salentin, S.; Haupt, V.J.; Schroeder, M. PLIP 2021: Expanding the scope of the protein-ligand interaction profiler to DNA and RNA. *Nucleic Acids Res.*, **2021**, 49(W1), W530-W534.
<http://dx.doi.org/10.1093/nar/gkab294> PMID: 33950214
- [75] Torres, P.H.M.; Sodero, A.C.R.; Jofily, P.; Silva-Jr, F.P. Key Topics in Molecular Docking for Drug Design. *Int. J. Mol. Sci.*, **2019**, 20(18), 4574.
<http://dx.doi.org/10.3390/ijms20184574> PMID: 31540192
- [76] Meng, X.Y.; Zhang, H.X.; Mezei, M.; Cui, M. Molecular docking: A powerful approach for structure-based drug discovery. *Curr. Computeraided Drug Des.*, **2011**, 7(2), 146-157.
<http://dx.doi.org/10.2174/157340911795677602> PMID: 21534921
- [77] Owoloye, A.J.; Ligali, F.C.; Enejoh, O.A.; Musa, A.Z.; Aina, O.; Idowu, E.T. Molecular docking, simulation and binding free energy analysis of small molecules as PHT1 inhibitors. *PLoS One*, **2022**, 17(8), e0268269.
<http://dx.doi.org/10.1371/journal.pone.0268269> PMID: 36026508
- [78] Hang, Z.; Zhou, L.; Xing, C.; Wen, Y.; Du, H. The blood-brain barrier, a key bridge to treat neurodegenerative diseases. *Ageing Res. Rev.*, **2023**, 91, 102070.
<http://dx.doi.org/10.1016/j.arr.2023.102070> PMID: 37704051
- [79] Dartois, V.A.; Rubin, E.J. Anti-tuberculosis treatment strategies and drug development: Challenges and priorities. *Nat. Rev. Microbiol.*, **2022**, 20(11), 685-701.
<http://dx.doi.org/10.1038/s41579-022-00731-y> PMID: 35478222
- [80] Griego, A.; Scarpa, E.; De Matteis, V.; Rizzello, L. Nanoparticle delivery through the BBB in central nervous system tuberculosis. *Ibrain*, **2023**, 9(1), 43-62.
<http://dx.doi.org/10.1002/ibra.12087> PMID: 37786519
- [81] Olson, R.D.; Assaf, R.; Brettin, T.; Conrad, N.; Cucinell, C.; Davis, J.J.; Dempsey, D.M.; Dickerman, A.; Dietrich, E.M.; Kenyon, R.W.; Kuscuoğlu, M.; Lefkowitz, E.J.; Lu, J.; Machi, D.; Macken, C.; Mao, C.; Niewiadomska, A.; Nguyen, M.; Olsen, G.J.; Overbeek, J.C.; Parrello, B.; Parrello, V.; Porter, J.S.; Pusch, G.D.; Shukla, M.; Singh, I.; Stewart, L.; Tan, G.; Thomas, C.; VanOeffelen, M.; Vonstein, V.; Wallace, Z.S.; Warren, A.S.; Wattam, A.R.; Xia, F.; Yoo, H.; Zhang, Y.; Zmasek, C.M.; Scheuermann, R.H.; Stevens, R.L. Introducing the bacterial and viral bioinformatics resource center (BV-BRC): A resource combining PATRIC, IRD and ViPR. *Nucleic Acids Res.*, **2023**, 51(D1), D678-D689.
<http://dx.doi.org/10.1093/nar/gkac1003> PMID: 36350631
- [82] Bolognesi, M.L.; Cavalli, A. Multitarget drug discovery and polypharmacology. *ChemMedChem*, **2016**, 11(12), 1190-1192.
<http://dx.doi.org/10.1002/cmdc.201600161> PMID: 27061625
- [83] Aguilera, E.; Varela, J.; Birriel, E.; Serna, E.; Torres, S.; Yaluff, G.; de Bilbao, N.V.; Aguirre-López, B.; Cabrera, N.; Díaz Mazariegos, S.; de Gómez-Puyou, M.T.; Gómez-Puyou, A.; Pérez-Montfort, R.; Minini, L.; Merlino, A.; Cerecetto, H.; González, M.; Alvarez, G. Potent and selective inhibitors of *Trypanosoma cruzi* triosephosphate isomerase with concomitant inhibition of cruzipain: Inhibition of parasite growth through multitarget activity. *ChemMedChem*, **2016**, 11(12), 1328-1338.
<http://dx.doi.org/10.1002/cmdc.201500385> PMID: 26492824
- [84] Sidorov, P.; Desta, I.; Chessé, M.; Horvath, D.; Marcou, G.; Varnek, A.; Davioud-Charvet, E.; Elhabiri, M. Redox polypharmacology as an emerging strategy to combat malarial parasites. *ChemMedChem*, **2016**, 11(12), 1339-1351.
<http://dx.doi.org/10.1002/cmdc.201600009> PMID: 26947575
- [85] Bottegoni, G.; Veronesi, M.; Bisignano, P.; Kacker, P.; Favia, A.D.; Cavalli, A. Development and application of a virtual screening protocol for the identification of multitarget fragments. *ChemMedChem*, **2016**, 11(12), 1259-1263.
<http://dx.doi.org/10.1002/cmdc.201500521> PMID: 26663255
- [86] Molodtsov, V.; Scharf, N.T.; Stefan, M.A.; Garcia, G.A.; Murakami, K.S. Structural basis for rifamycin resistance of bacterial RNA polymerase by the three most clinically important RpoB mutations found in *Mycobacterium tuberculosis*. *Mol. Microbiol.*, **2017**, 103(6), 1034-1045.
<http://dx.doi.org/10.1111/mmi.13606> PMID: 28009073
- [87] Telenti, A.; Imboden, P.; Marchesi, F.; Matter, L.; Schopfer, K.; Bodmer, T.; Lowrie, D.; Colston, M.J.; Cole, S. Detection of rifampicin-resistance mutations in *Mycobacterium tuberculosis*. *Lancet*, **1993**, 341(8846), 647-651.
[http://dx.doi.org/10.1016/0140-6736\(93\)90417-F](http://dx.doi.org/10.1016/0140-6736(93)90417-F) PMID: 8095569
- [88] Madadi, A.K.; Sohn, M.J. Comprehensive therapeutic approaches to tuberculous meningitis: Pharmacokinetics, combined dosing, and advanced intrathecal therapies. *Pharmaceutics*, **2024**, 16(4), 540.
<http://dx.doi.org/10.3390/pharmaceutics16040540> PMID: 38675201
- [89] Talluri, S. Computational design of drugs for Epilepsy using a novel guided evolutionary algorithm for enhanced Blood Brain Barrier permeability. *ChemRxiv*, **2024**, 2, 1-24.
<http://dx.doi.org/10.26434/chemrxiv-2024-bfgk0>
- [90] Mhambi, S.; Fisher, D.; Tchokonte, M.B.T.; Dube, A. Permeation challenges of drugs for treatment of neurological tuberculosis and HIV and the application of magneto-electric nanoparticle drug

- delivery systems. *Pharmaceutics*, **2021**, 13(9), 1479.
<http://dx.doi.org/10.3390/pharmaceutics13091479> PMID: 34575555
- [91] Dong, X. Current strategies for brain drug delivery. *Theranostics*, **2018**, 8(6), 1481-1493.
<http://dx.doi.org/10.7150/thno.21254> PMID: 29556336
- [92] Zhang, Q.; An, X.; Liu, H.; Wang, S.; Xiao, T.; Liu, H. Uncovering the resistance mechanism of *Mycobacterium tuberculosis* to rifampicin due to RNA polymerase H451D/Y/R mutations from computational perspective. *Front Chem.*, **2019**, 7, 819.
<http://dx.doi.org/10.3389/fchem.2019.00819> PMID: 31850310
- [93] Zhang, Q.; Tan, S.; Xiao, T.; Liu, H.; Shah, S.J.A.; Liu, H. Probing the molecular mechanism of rifampin resistance caused by the point mutations S456L and D441V on *Mycobacterium tuberculosis* RNA polymerase through gaussian accelerated molecular dynamics simulation. *Antimicrob. Agents Chemother.*, **2020**, 64(7), e02476-19.
<http://dx.doi.org/10.1128/AAC.02476-19> PMID: 32393493
- [94] Ali, E.Z.; Hamidon, N.H.; Issa, R. *In silico* mutational analysis in RNA polymerase β subunit (rpoB) gene of rifampicin-resistant in *Mycobacterium tuberculosis* from Malaysia. *AsPac J. Mol. Biol. Biotechnol.*, **2021**, 29(3), 47-58.
- [95] Morphy, R.; Kay, C.; Rankovic, Z. From magic bullets to designed multiple ligands. *Drug Discov. Today*, **2004**, 9(15), 641-651.
[http://dx.doi.org/10.1016/S1359-6446\(04\)03163-0](http://dx.doi.org/10.1016/S1359-6446(04)03163-0) PMID: 15279847
- [96] Gygli, S.M.; Borrell, S.; Trauner, A.; Gagneux, S. Antimicrobial resistance in *Mycobacterium tuberculosis*: Mechanistic and evolutionary perspectives. *FEMS Microbiol. Rev.*, **2017**, 41(3), 354-373.
<http://dx.doi.org/10.1093/femsre/fux011> PMID: 28369307